Available online at www.sciencedirect.com
SCIENCE DIRECT®
Journal of Contaminant Hydrology 62–63 (2003) 675–694
JOURNAL OF Contaminant Hydrology
www.elsevier.com/locate/jconhyd

Transport of a reactive tracer in saturated alluvium described using a three-component cation-exchange model

Enid J. Sullivan[1], Paul W. Reimus*, Dale A. Counce[2]

Los Alamos National Laboratory, P.O. Box 1663, MS J534, Los Alamos, NM 87545, USA

Abstract

A weakly sorbing cation, lithium, will be used as a reactive tracer in upcoming field tracer tests in the saturated alluvium south of Yucca Mountain, Nevada. One objective of the field tests is to determine how well field-scale reactive transport can be predicted using transport parameters derived from laboratory experiments. This paper describes several laboratory lithium batch sorption and column transport experiments that were conducted using ground water and alluvium obtained from the site of the planned field tests. In the batch experiments, isotherms were determined over 2.5 orders of magnitude of lithium concentrations, corresponding to the range expected in the field tests. In addition to measuring equilibrium lithium concentrations, concentrations of other cations, namely Na^+, K^+, and Ca^{2+}, were measured in the batch tests to determine Li^+-exchangeable equilibria. This information was used in conjunction with alluvium cation exchange capacity measurements to parameterize a three-component cation-exchange model (EQUIL) that describes lithium sorption in the alluvium system. This model was then applied to interpret the transport behavior of lithium ion in saturated alluvium column tests conducted at three different lithium bromide injection concentrations. The concentrations were selected such that lithium ion either dominated, accounted for a little over half, or accounted for only a small fraction of the total cation equivalents in the injection solution. Although tracer breakthrough curves differed significantly under each of these conditions, with highly asymmetric responses occurring at the highest injection concentrations, the three-component cation-exchange model reproduced the observed transport behavior of lithium and the other cations in each case with a similar set of model parameters. In contrast, a linear K_d-type sorption model could only match the lithium responses at the lowest injection concentration. The

* Corresponding author. Tel.: +1-505-665-2537; fax: +1-505-665-9118.
E-mail addresses: ejs@lanl.gov (E.J. Sullivan), preimus@lanl.gov (P.W. Reimus), counce@lanl.gov (D.A. Counce).
[1] Fax: +1-505-665-9118.
[2] Fax: +1-505-665-3285.

doi:10.1016/S0169-7722(02)00182-1

three-component model will be used to interpret the field tests, with the expectation that it will help refine estimates of effective flow porosity, particularly if the lithium response curves are asymmetric.

Keywords: Cross-hole tracer test; Lithium; Column; Batch; MULTRAN; EQUIL

1. Introduction

Yucca Mountain, Nevada, located about 145 km northwest of Las Vegas, is the site of a potential high-level nuclear waste repository. It is currently undergoing extensive characterization and assessment to determine its suitability for such a role. Plans call for wastes emplaced within Yucca Mountain to be isolated from the accessible environment by a system of multiple barriers. Engineered barriers will consist of components within the repository itself, while a two-part geologic barrier will consist of the unsaturated tuff between the repository and the regional aquifer below, as well as the saturated-zone aquifer system extending from the repository to a ground-water discharge zone. The last geologic barrier that radionuclides will encounter is the saturated alluvium south of Yucca Mountain. Cross-hole hydraulic and tracer tests are being conducted in this alluvium. The objectives of cross-hole tracer tests include: (1) testing and validating a conceptual transport model in the saturated alluvium, (2) obtaining estimates of key transport parameters in the flow system, and (3) assessing the applicability of laboratory-derived tracer transport parameters to field-scale transport predictions.

The latter objective is important because radionuclides cannot be tested in the field, so favorable comparisons of laboratory- and field-scale transport of nonradioactive tracers can lend credibility to the practice of using laboratory-derived radionuclide transport parameters in field-scale predictive simulations. To satisfy this objective, the transport characteristics of a sorbing tracer must be determined in both the laboratory and the field to allow comparisons and cross-predictions between the two scales. Lithium ion, a weakly sorbing, cation-exchanging tracer, will be used for this purpose. Lithium has the advantages of being inexpensive, highly soluble, and nontoxic. It can be expected to move relatively quickly through an aquifer so that a positive response can be obtained in a reasonable time in a field test. Lithium ion can be considered as a reasonable surrogate for weakly sorbing radionuclides such as NpO_2^+ under oxidizing conditions (Turin et al., in press).

This paper presents the results and interpretations of several lithium laboratory transport experiments using ground water and alluvium obtained from the site of the planned field tracer tests (well NC-EWDP-19D, Fig. 1). These experiments included (1) batch sorption tests in which lithium sorption isotherms were determined over a range of lithium concentrations that are expected in the field, (2) cation exchange capacity (CEC) measurements, and (3) column transport tests in which lithium bromide was injected as a pulse at three different concentrations spanning the range expected in the field. A simplified three-component cation-exchange model coupled with a multicomponent numerical transport model, MULTRAN (multicomponent transport), was used to describe lithium transport through the columns. MULTRAN accounts for advection, dispersion, and

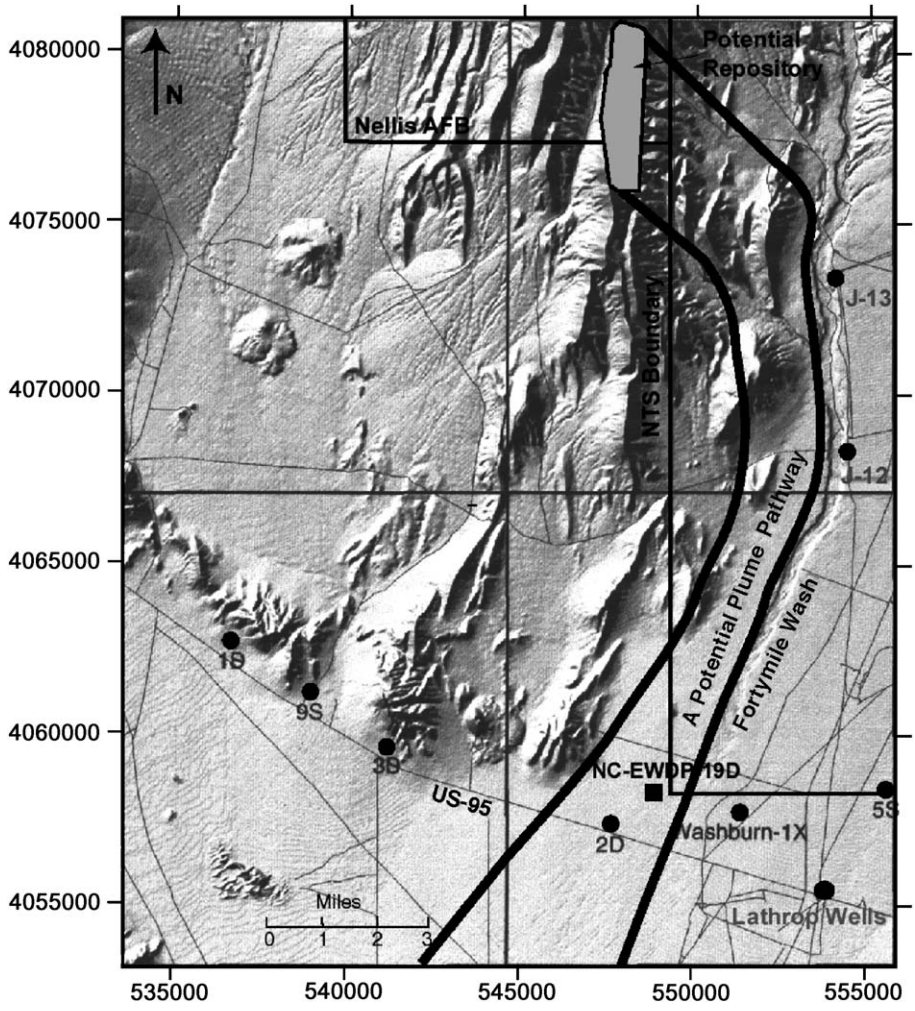

Fig. 1. Map showing location of well NC-EWDP-19D in relation to potential repository footprint and the Nevada Test Site. Circles are locations of other wells (UTM coordinates).

diffusion in either single- or dual-porosity systems while maintaining cation exchange equilibria and local charge balance as species are transported.

Several previous studies have employed multicomponent, cation exchange approaches to describe reactive transport in porous media (Callahan et al., 2000 provides a detailed listing). Of these, Valocchi et al. (1981a,b) provided a fundamental analysis of the cation exchange process, or ion chromatography, when water is injected into an aquifer, and discussed a model for this process. Later, Appelo et al. (for example, Appelo and Postma, 1993; Appelo, 1994, 1996) discussed the cation exchange principles and derived specific equations for multicomponent problems under the framework of salinization. Lichtner (1995) and Callahan et al. (2000) discuss models and tracer studies similar to those described in this

paper, except that they were conducted in fractured tuffaceous rock. Reviews of multi-component transport models are found in Liu and Narasimhan (1989), Yeh and Tripathi (1989), and Lichtner (1996). Predictive models such as HYDROGEOCHEM (Yeh and Tripathi, 1988), PHREEQC (Parkhurst, 1995), FEREACT (TebesStevens et al., 1998), and FEHM (Robinson et al., 2000) have been used to describe multiple-species transport in geologic media. The modeling approach presented in this paper is a practical simplification of these models in that it accounts only for the cation exchange reactions necessary to describe the transport of solutes of interest in the alluvium column experiments. Cation exchange was selected because it is the major mechanism affecting Li^+ transport in the alluvial systems of interest. This avoids multiple fitting parameters and resulting non-unique curve fits. Complexation was not expected in the types of water and geomaterials used, and the tracer, a monovalent cation, was selected to minimize this effect.

2. Materials and methods

2.1. Water and alluvium

All experiments were conducted using ground water batches collected from well NC-EWDP-19D (Fig. 1) in June 2000 or November 2000. The batches had slightly different chemistries because they were collected from different depth intervals (Table 1). Batch 1 was used for all experiments except the column experiments with the intermediate LiBr injection concentration. Both waters are essentially sodium bicarbonate waters that are nearly saturated with respect to silica and with a pH greater than 8. The ground water was filter-sterilized using a 0.2-μm filter before use.

The alluvium used in the experiments is from drill cuttings obtained from NC-EWDP-19D at depth intervals of 124–126 and 127–129 m below ground surface (bgs), approximately 15 to 23 m below the water table. Cuttings samples were wet-sieved using

Table 1
Major ion chemistry of NC-EWDP-19D water used in the experiments

Species	Batch 1 (mg/l)	Batch 2 (mg/l)
Ca^{2+}	2.2	7.5
Na^+	118	75.5
K^+	5.2	4.1
Mg^{2+}	1.13	0.65
Li^+	0.15	0.09
Si	52.5	27.1
HCO_3^-	193	168
CO_3^{2-}	43.8	0
SO_4^{2-}	25.9	23.0
Cl^-	5.7	5.6
F^-	2.1	1.8
pH	9.2	8.1

Batch 1 was collected in June 2000 from an open borehole. Batch 2 was collected from two isolated screened intervals in the upper 150 ft of the saturated zone. This batch was used only for the 0.006 M LiBr column experiments.

a synthetic $NaHCO_3$ well water in the laboratory (ASTM, 1999), and the size range between 75 and 2000 μm was retained for testing. Material from the two intervals was combined in a 50:50 mass ratio for the column experiments because there was not enough material from the individual intervals to pack the columns. Table 2 gives the bulk mineralogy of the alluvium from the two intervals as determined by quantitative X-ray diffraction (QXRD) (Chipera and Bish, 1995). Table 2 also lists the surface area of the samples determined by a single-point Brunauer–Emmett–Teller (BET) nitrogen adsorption/desorption method (Brunauer et al., 1938). Smaller size fractions were excluded from the column experiments because clogging and pressure buildup occurs in the column end frits and flow lines otherwise. In the batch studies, fine fractions were tested in parallel with the large fractions used in the columns to provide some measure of the effect that clays and fine particles have on the sorption process. Previous work indicates that zeolite predominates over clays in interactions with Li^+ in these materials (Sullivan et al., 2001). Zeolite was found in similar quantity in both size fraction sets.

2.2. Cation-exchange capacity (CEC) measurements

Cation exchange capacities were measured for the alluvium from the two different intervals and the same sieve size fraction as used for the column studies. CECs were measured using a three-step process of saturating the alluvium surface sites with lithium ion, modified from that of Ming and Dixon (1987). Half-gram samples of alluvium were placed in contact with ~ 30 ml of 1 M LiBr solution prepared in deionized water. The alluvium-solution mixture was shaken for at least 1 h, centrifuged, and the supernatant was decanted off into a collection container. This treatment was repeated two more times, with the supernatant from each step being combined with that from the previous steps. The final solution (~ 90 ml) was analyzed for Na^+, Ca^{2+}, K^+, and Mg^{2+} using inductively coupled plasma-atomic emission spectrometry (ICP-AES) to determine the total number of equivalents of cations that lithium had displaced from the alluvium surfaces. This total number of

Table 2
Mineralogy (wt.%) and surface area of NC-EWDP-19D alluvium samples used in batch sorption and column experiments

Mineral	124–126 m bgs	127–129 m bgs
Smectite	4 ± 1	6 ± 2
Clinoptilolite	7 ± 1	6 ± 1
Kaolinite	1 ± 1	1 ± 1
Mica	1 ± 1	trace
Tridymite	5 ± 1	6 ± 1
Cristobalite	13 ± 1	16 ± 1
Quartz	17 ± 1	20 ± 2
Feldspar	53 ± 8	44 ± 6
Calcite	–	1 ± 1
Hematite	1 ± 1	trace
Hornblende	–	–
BET surface area (m^2/g)	5.34	5.64

equivalents divided by the mass of alluvium is the cation exchange capacity of the alluvium, expressed as eq/kg or meq/g.

It is well known that cation exchange capacities of materials are dependent on the cation used to saturate the material surfaces (Anghel et al., in press). Cs^+ is often used to obtain a measure of the "total" CEC of a material because Cs^+ sorbs very strongly to mineral surfaces and will displace most exchangeable cations encountered in nature. To obtain an estimate of the Cs^+-exchangeable CEC, the above procedure was repeated on each of the half-gram alluvium samples that had been subjected to LiBr solution treatments using 1 M CsCl as the saturating solution. However, the CEC determined from the lithium saturation steps was the value used in subsequent modeling of the batch sorption and column experiments because only cations displaced by lithium were judged to be of practical interest when lithium is the sorbing species.

2.3. Batch sorption experiments

Separate lithium batch sorption experiments were conducted on the sieved material from each of the two depth intervals that were eventually combined for the column experiments. Duplicate measurements were conducted at starting lithium concentrations of approximately 1, 3, 10, 30, 100, and 300 mg/l Li^+ for each material to obtain a sorption isotherm over a 2.5-order-of-magnitude range of concentrations. Starting solutions were prepared by dissolving a known mass of LiBr in a known volume of NC-EWDP-19D well water and then diluting by weight with well water to the desired starting concentrations. In all of the batch tests, 20 ml of lithium solution was placed in contact with approximately 5 g of alluvium material in 50-ml polycarbonate Oak Ridge centrifuge tubes that were shaken for 48 h on an orbital shaker. Separate control samples (lithium-spiked solutions in centrifuge tubes without any alluvium material) and blanks (non-spiked well water in contact with alluvium) were processed in parallel with the tubes containing both lithium and alluvium. The controls were used to verify that lithium sorption to tube walls was insignificant, and the blanks were used to measure any lithium background that might be leached out of the alluvium samples. After shaking, the tubes were centrifuged at $30{,}000 \times g$ for 1 h, and then an aliquot of supernatant was pipetted off for cation and bromide analyses. Cations (Li^+, Na^+, K^+, Ca^{2+}, and Mg^{2+}) were analyzed by ICP-AES and bromide was analyzed by liquid chromatography. Chromatography conditions included a Dionex AS14A column, 8 mM Na_2CO_3/1 mM $NaHCO_3$ mobile phase at 0.5 ml/min, ASRS suppression, and conductivity detection.

The starting lithium concentration for each measurement was determined from both the corresponding bromide and lithium concentrations in the control samples. In general, lithium concentrations measured in the control samples were in good agreement with those determined from the bromide measurements, indicating that lithium sorption to centrifuge tube walls was negligible. The mass of lithium sorbed per unit mass of alluvium material was determined by difference.

2.4. Column transport experiments

Column experiments were conducted in duplicate using separate 30 cm long by 2.5-cm diameter glass columns equipped with PTFE end fittings, including a 20-μm end frit and

PTFE tubing. Each column was pre-soaked in deionized water to remove any residual ions. The columns were packed dry with a 50:50 mass ratio of the wet-sieved alluvium from the two intervals that were used in batch sorption and CEC testing. The columns were then saturated by flushing with deaerated ground water until air bubbles were no longer visible. They were also packed in ice for 8 h to promote oxygen and nitrogen dissolution in the water. The saturated vs. dry weights of the columns indicated a final porosity of about 40% with a pore volume of about 60 ml in each column.

Three transport experiments were conducted in each column at a flow rate of approximately 10 ml/h, with the two columns run in parallel. Each experiment involved the injection of approximately one pore volume of a tracer solution containing LiBr and 2 mg/l of a fluorinated benzoate (either pentafluorobenzoate or 2,4-difluorobenzoate) dissolved in NC-EWDP-19D ground water. The experiments differed in the concentrations of LiBr in the injection pulses. The first duplicate set of experiments was conducted using an injection concentration of 0.029 M LiBr (200 mg/l Li^+), the second set had a concentration of 0.0013 M LiBr (9 mg/l Li^+), and the third set had a concentration of 0.006 M LiBr (42 mg/l Li^+). These concentrations were selected so that Li^+ dominated the cation equivalents in solution in the first case (91% of total cation equivalents), was a relatively minor fraction of the total cation equivalents in the second case (24%), and accounted for about half of the cation equivalents in the third case (61%). These three situations represent a range of conditions that will likely occur during field testing, with relatively high concentrations present near the injection well immediately after injection and concentrations decreasing as the tracer pulse advects and disperses through the flow system.

The tracer solutions were injected simultaneously into the two columns using a syringe pump (Harvard Systems). After one pore volume of tracer was injected, tracer-free ground water was injected at 10 ml/h using a piston pump (SciLog). Column effluent samples were collected using an automatic fraction collector (Gilson) set up to collect samples simultaneously from both columns in tared test tubes at pre-set time intervals. The samples were analyzed for the same cations (Li^+, Na^+, K^+, Ca^{2+}, and Mg^{2+}) that were analyzed in the batch sorption experiments using ICP-AES. Bromide and the fluorinated benzoates were analyzed by liquid chromatography, with the latter being quantified by UV absorption. Samples were diluted as necessary for the tracer analyses.

3. Modeling approach

3.1. Batch sorption experiments

Batch sorption data were used to develop Q values that were subsequently compared with Q values from the column tests (see Experimental results and analyses). Because equilibrium data are not linear with solution concentration, several batch points are measured to accommodate the changes in the concentration of the sorbing tracer (here, Li^+). This range of concentrations is selected to approximate the range of values that would be used in the field during a tracer test, or expected after dilution. Multicomponent modeling better describes systems in which a cation such as Li^+ comprises a large

percentage of the cation equivalents in solution, similar to what would be expected during a tracer test.

We established in the batch sorption experiments that only two cations, Na^+ and Ca^{2+}, exchanged significantly with Li^+ (see Experimental results and analyses). K^+ was exchanged to a minor degree, but the amount was so small relative to Na^+ and Ca^{2+} that it was considered reasonable to lump the K^+ with the Na^+ as a generic "monovalent cation". Thus, a simplified three-component cation-exchange model was used to interpret the batch experiments. The generic exchange reactions were assumed to be:

$$\begin{aligned} &A + BX \Rightarrow AX + B \\ &2A + CX_2 \Rightarrow 2AX + C \\ &2B + CX_2 \Rightarrow 2BX + C \end{aligned} \tag{1}$$

where A and B = monovalent cations (Li^+ and $Na^+ + K^+$ for this study), C = divalent cation (Ca^{2+} for this study), and X = a monovalent negatively charged surface site.

Reactions (1) have the following corresponding mass-action expressions, which were solved simultaneously along with the total surface cation balance equation:

$$Q_1 = \frac{[AX][B]}{[A][BX]} \tag{2a}$$

$$Q_2 = \frac{[AX]^2[C]}{[A]^2[CX_2]} \tag{2b}$$

$$\frac{Q_2}{Q_1^2} = \frac{[BX]^2[C]}{[B]^2[CX_2]} \tag{2c}$$

$$\mathrm{CEC} = \frac{\phi}{\rho_B}([AX] + [BX] + 2[CX_2]) \qquad \text{(surface cation balance)} \tag{3}$$

where $[i]$ = concentration of species i (mol/l of solution); Q_i = dimensionless ion exchange constant; CEC = cation exchange capacity measured with lithium ion (eq/kg); ρ_B = bulk density of rock (kg/l of bulk rock); and ϕ = porosity.

The Q_i values should not be confused with equilibrium constants, as they are defined in terms of species concentrations, not activities. Eqs. (2a)–(2c) and (3) thus represent a nonstandard mass-action convention that ignores activity coefficients and uses solution volume (rather than rock mass) as the basis for surface species concentrations (mol/l). The more standard Gaines–Thomas convention for Eqs. (2a)–(2c) and (3) (Appelo and Postma, 1993), in which [AX], [BX], and $[CX_2]$ represent equivalent fractions (eq/kg divided by CEC), can be obtained by multiplying both sides of Eqs. (2b) and (2c) by $\rho_B/2\phi$(CEC), dividing both sides of Eq. (3) by CEC, and multiplying the right-hand side of Eq. (3) by ρ_B/ϕ. In this case, the "selectivity" or "exchange" coefficients for the

displacement of Li^+ and Ca^{2+} by Na^+ under the Gaines–Thomas convention (Appelo and Postma, 1993) are $\frac{1}{Q_1}$ and $\frac{1}{Q_1}\sqrt{\frac{Q_2\rho_B}{2\phi(CEC)}}$, respectively.

A simple FORTRAN program called EQUIL_FIT was used to obtain the best simultaneous fit to the Li^+, Na^+, and Ca^{2+} data obtained in the batch sorption experiments using Q_1 and Q_2 as adjustable parameters. The CEC was set equal to the lithium cation exchange capacity of the alluvium. The fits were optimized by minimizing the sum of squares of differences between the logarithms of the model-predicted concentrations and the experimental concentrations. Logarithms were used in the optimization algorithm so that the fits would not be biased toward the data obtained at the highest lithium concentrations. A similar process can be found in Appelo (1994).

3.2. Column transport experiments

The column transport experiments were interpreted using a FORTRAN program called MULTRAN (multicomponent transport). MULTRAN is a two-dimensional numerical model that employs an implicit-in-time, alternating-direction finite-difference method to solve the equations describing multicomponent transport of sorbing and nonsorbing solutes in a single- or dual-porosity medium. Fig. 2 illustrates the assumed model domain and shows an example of the spatial discretization. Advective transport, simulated by solving the advection–dispersion equation, is assumed to occur only in the x-direction in region I. The first and last nodes in the x-direction in this region are modeled as well-mixed regions that simulate either boreholes in field experiments or flow manifolds in laboratory experiments. Reinjection of part or all of the solution entering the last node back into the first node can be specified to simulate recirculating conditions in tracer experiments. Only diffusive transport is assumed to occur in the y-direction in both regions I and II, with the model having the capability to simulate different diffusion coefficients in the different regions. Finally, within each region, additional diffusive transport can be simulated into "grains", which are assumed to be spherical. These grains can be assigned a lognormal distribution of diameters with specified mean and variance. The user can control the spatial discretization within each region and within the grains. The user can also eliminate certain portions of the model domain shown in Fig. 2 simply by specifying that they have zero porosity. For instance, if one wishes to simulate a single-porosity medium, it is only necessary to specify a zero porosity for region II and zero porosity for the grains in region I. This approach was taken to simulate the column transport experiments conducted in this study because the columns were packed with a relatively uniform alluvium material that had no apparent secondary porosity. Thus, the model domain was effectively reduced to a one-dimensional system (region I), which greatly simplified numerical computations.

Each time step of a MULTRAN simulation is broken into four computational segments that are conducted sequentially.

(1) Solution of the advection–dispersion equation in the x-direction in region I:

$$\frac{\partial c}{\partial t} = -V\frac{\partial c}{\partial x} + D\frac{\partial^2 c}{\partial x^2} \tag{4}$$

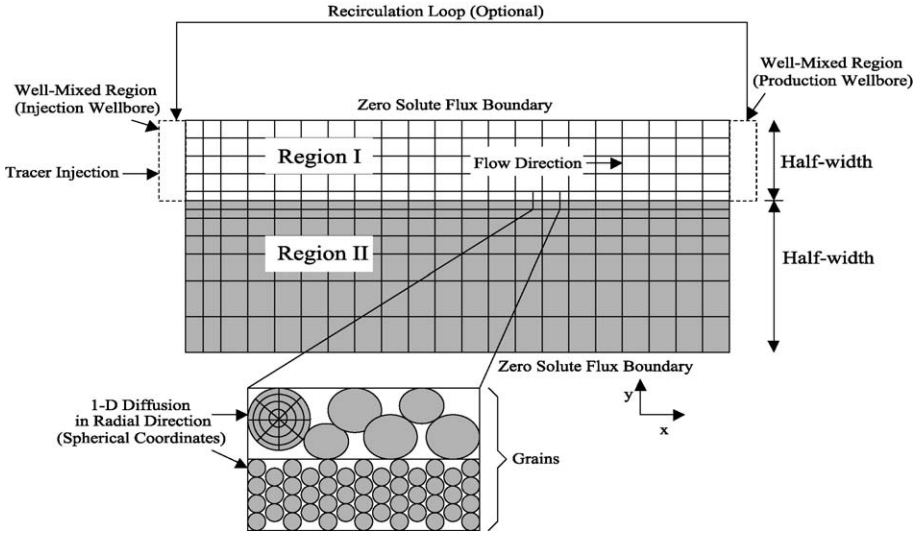

Fig. 2. Schematic illustration of MULTRAN model domain. Blocks are finite-difference cells that are solved at their midpoints. Region I is the high-permeability layer (advective transport in x-direction, diffusive in y-direction), region II is the low-permeability layer (diffusive transport in y-direction only).

where c = molar concentration (mol/l); V = velocity in x-direction (cm/s); and D = dispersion coefficient (cm^2/s) ($D = \alpha V$, α = dispersivity).

(2) Solution of the multicomponent diffusion equation(s) and the local electroneutrality equation in the y-direction in regions I and II (coupled):

Multicomponent diffusion equation for all species except species n (Newman, 1973)

$$\frac{\partial c_i}{\partial t} = D_i \nabla^2 c_i - \sum_j \frac{z_j}{z_i}(D_j - D_n)\nabla(t_i \nabla c_i) \tag{5}$$

where c_i = molar concentration of species i (mol/l); D_i = diffusion coefficient of species i (cm^2/s); ∇ = del operator; ∇^2 = Laplacian operator; $t_i = \frac{z_i^2 u_i c_i}{\sum_j z_j^2 u_j c_j}$ = transference number of species i; z_i = charge of species i; $u_i = D_i/RT$ = mobility of species i, where R = gas constant and T = temperature (K).

Electroneutrality equation for species n

$$z_n c_n = -\sum_{j \neq n} z_j c_j \tag{6}$$

(3) Solution of the multicomponent diffusion equation(s) and the local electroneutrality equation in the radial direction in the grains of both regions I and II (same as step 2, but using spherical coordinates).

(4) Chemical re-equilibration of the entire system with respect to cation exchange. This step is accomplished by solving Eqs. (2a)–(2c) and (3) at each node in the model domain to ensure that the equilibrium expressions and the surface cation balance are locally satisfied. The system is assumed to be always at chemical equilibrium (i.e., reaction kinetics assumed to be fast relative to transport rates). Slow-reaction kinetics may be considered in a future version of MULTRAN.

The second and third steps described above were not needed for this study because of the assumption of one-dimensional, single-porosity transport (no diffusion into grains or into non-flowing porosity). These steps are included here, however, for completeness because it was not evident until after the first experiments were conducted that diffusive mass transfer into non-flowing regions was not important in the columns. The full two-dimensional capabilities of MULTRAN are used to interpret a field experiment in a fractured volcanic tuff described in another paper in this issue (Reimus et al., 2003, this issue).

4. Experimental results and analyses

4.1. Cation exchange capacity measurements

The lithium cation exchange capacities of the two alluvium intervals were essentially the same, with the upper interval (124–126 m bgs) having a Li^+ CEC value of 0.070 eq/kg, and the lower interval (127–129 m bgs) having a value of 0.089 eq/kg. The Cs^+ CEC values for these two intervals were 0.258 and 0.231 eq/kg, respectively. However, as stated above, only the lithium CEC results were used to interpret the batch sorption and column transport tests because only cations displaced by lithium are of practical interest in these experiments.

4.2. Batch sorption experiments

Figs. 3 and 4 show the lithium sorption isotherms with the [sodium + potassium] and calcium ion concentrations (after lithium sorption) for the two alluvium intervals tested.

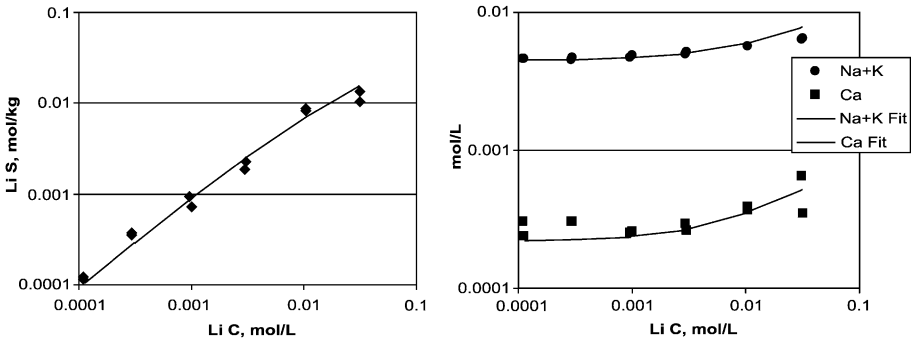

Fig. 3. Lithium sorption isotherm and concentrations of other cations in solution as a function of final lithium concentration for alluvium from 124–126 m bgs at NC-EWDP-19D. Cation exchange parameters corresponding to the model fits are listed in Table 3.

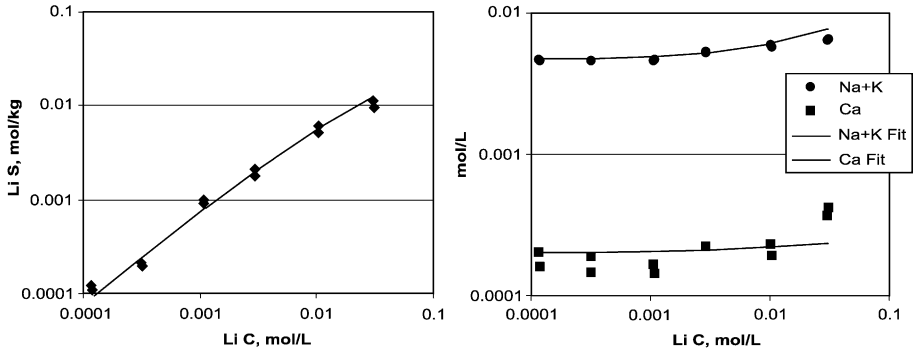

Fig. 4. Lithium sorption isotherm and concentrations of other cations in solution as a function of final lithium concentration for alluvium from 127–129 m bgs at NC-EWDP-19D. Cation exchange parameters corresponding to the model fits are listed in Table 3.

Potassium exchange with lithium was almost negligible, so potassium was combined with sodium to create a generic monovalent cation for interpretive purposes. Figs. 3 and 4 also show the best fits to the data obtained by the EQUIL_FIT code while holding the lithium CEC value for each alluvium interval to their measured values. The resulting best-fitting Q_1 and Q_2 values for the two alluvium intervals are listed in Table 3. It should be noted that there is considerable non-uniqueness to the fits when the CEC value is allowed to float. It was therefore important to obtain an independent measurement of the CEC value to constrain the fitting procedure.

4.3. Column transport experiments

The breakthrough curves of Br^-, Li^+, Na^+, and Ca^{2+}, expressed as meq/l vs. volume eluted through the columns, are shown in Figs. 5–7, for the experiments conducted at each of the three LiBr injection concentrations (shown in order from highest to lowest concentration). These figures also show the MULTRAN fits to each data set. The fluorinated benzoate data is not shown in these figures because it was essentially identical to the bromide data when normalized to the number of equivalents injected. The MULTRAN model parameters resulting in the best fits shown in Figs. 5–7 are

Table 3
Best-fitting Q_1 and Q_2 values for lithium ion exchange with the alluvium samples used in the experiments

Exchange parameter	124–126 m bgs	127–129 m bgs	Average[a]
CEC[b], eq/kg	0.07	0.089	0.0795
Q_1	0.060	0.039	0.0495
Q_2	0.092	0.136	0.114

[a] The average should be representative of the material used to pack the columns.
[b] CEC was measured, not fitted.

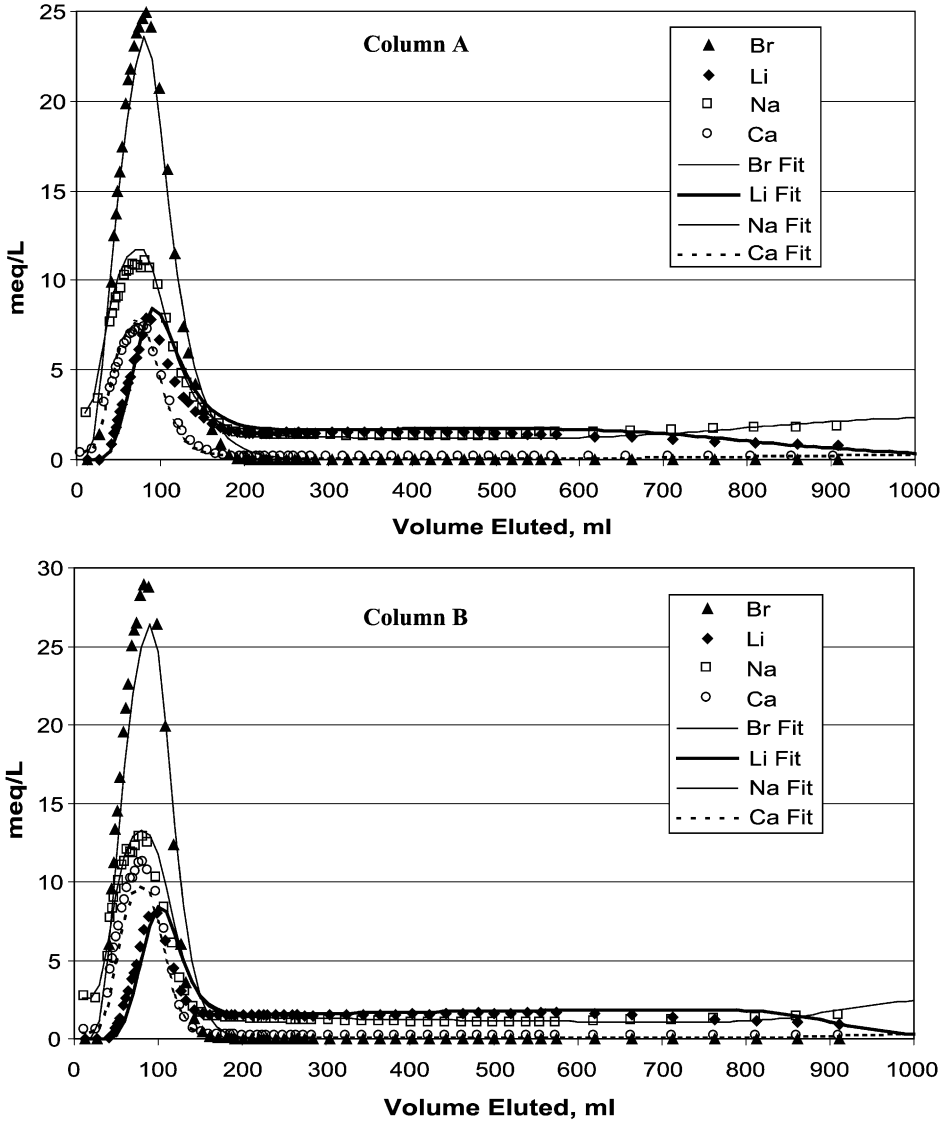

Fig. 5. Column data and MULTRAN fits for experiments with a LiBr injection concentration of 0.029 M, flow rate 10 ml/h.

listed in Table 4. The lithium CEC was fixed to 0.08 eq/kg for all of the experiments (the average value for the two intervals, which was taken to represent the CEC of the combined material), and Q_1 and Q_2 were adjusted to fit the data. The dispersivity in the column was also adjusted to obtain a reasonable fit to the bromide response curve. The fits were found to be quite sensitive to the background concentrations assumed in

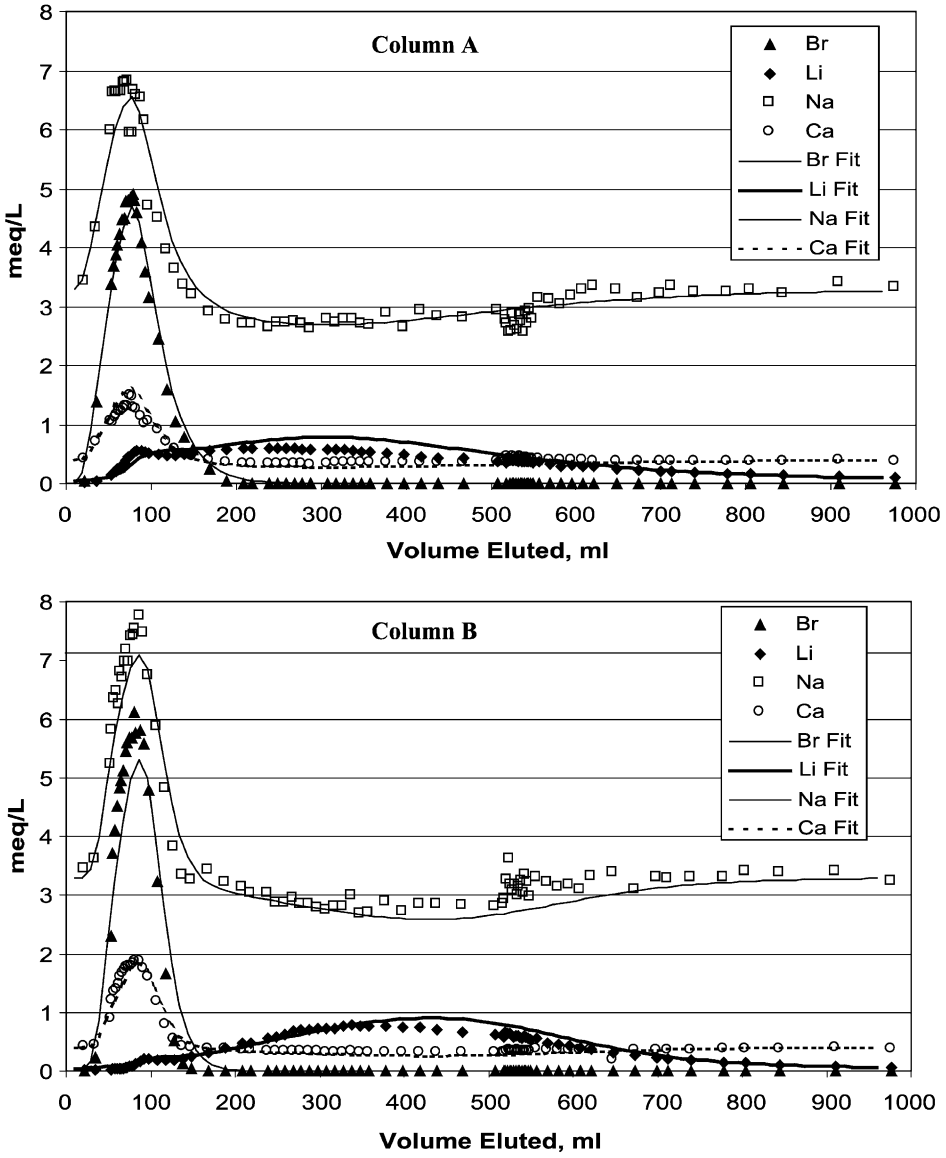

Fig. 6. Column data and MULTRAN fits for experiments with a LiBr injection concentration of 0.006 M, flow rate 10 ml/h.

the simulations, which were variable in the experiments because the columns were re-used to conduct subsequent experiments and residual concentrations of the cations varied somewhat. As Tables 3 and 4 indicate, the best-fitting ion exchange constants, Q_1 and Q_2, for the initial experiments in each column (0.029 M LiBr) were in very

Table 4
MULTRAN model parameters associated with the fits to the column transport data shown in Figs. 5–7

Experiment	Dispersivity (cm)	Q_1	Q_2
0.029 M LiBr, Column A (Fig. 5)	5.4	0.055	0.12
0.029 M LiBr, Column B (Fig. 5)	1.8	0.045	0.105
0.006 M LiBr, Column A (Fig. 6)	5.4	0.104	0.083
0.006 M LiBr, Column B (Fig. 6)	1.8	0.104	0.083
0.0013 M LiBr, Column A (Fig. 7)	5.4	0.104	0.083
0.0013 M LiBr, Column B (Fig. 7)	1.8	0.104	0.083

The lithium CEC value was assumed to be 0.08 eq/kg for all simulations.

good agreement with the values obtained from the batch experiments. In the subsequent column experiments, the best-fitting Q_1 values were about two times greater than in the batch experiments, and the best-fitting Q_2 values were just slightly lower than in the batch experiments. However, the same set of Q_1 and Q_2 values provided very good fits to the data from each of the last four column experiments (two experiments in each column).

5. Discussion and conclusions

5.1. Model fits

Examination of the MULTRAN model fits shown in Figs. 5–7 indicates that the model describes well the transport behavior of the cations through the columns, even though the response curves varied significantly for the three different LiBr injection concentrations. Furthermore, the model parameters did not have to be changed significantly for the different injection concentrations to achieve good fits. In fact, after the first set of column experiments (conducted at the highest LiBr injection concentration), the same Q_1 and Q_2 values provided excellent fits to the subsequent data sets obtained with two different LiBr injection concentrations. This result suggests that the model accurately represented the transport processes occurring in the columns.

The fact that the best-fitting Q_1 and Q_2 values obtained from the first experiment in each column were in good agreement with the values obtained from the batch sorption experiments indicates that the three-component exchange model is very effective in describing cation exchange over a wide range of cation concentrations under both static and flowing conditions. The shift in Q_1 and Q_2 values after the first experiment suggests that there was a change in the cation exchange behavior of the alluvium material that caused a shift in either the effective CEC value of the material, the values of Q_1 and Q_2, or both. The field interval from which the column material was taken had water chemistry with a higher concentration of Ca^{2+} and a lower concentration of Na^{+} than the water that was used in the batch experiments and all but the last column experiment (Batch 1 in Table 1). Thus, the use of the Batch 1 water in the column experiments, combined with the very high Li^{+} concentration used in the first experiment, may have resulted in a shift in the effective parameters of the column material. Irreversible

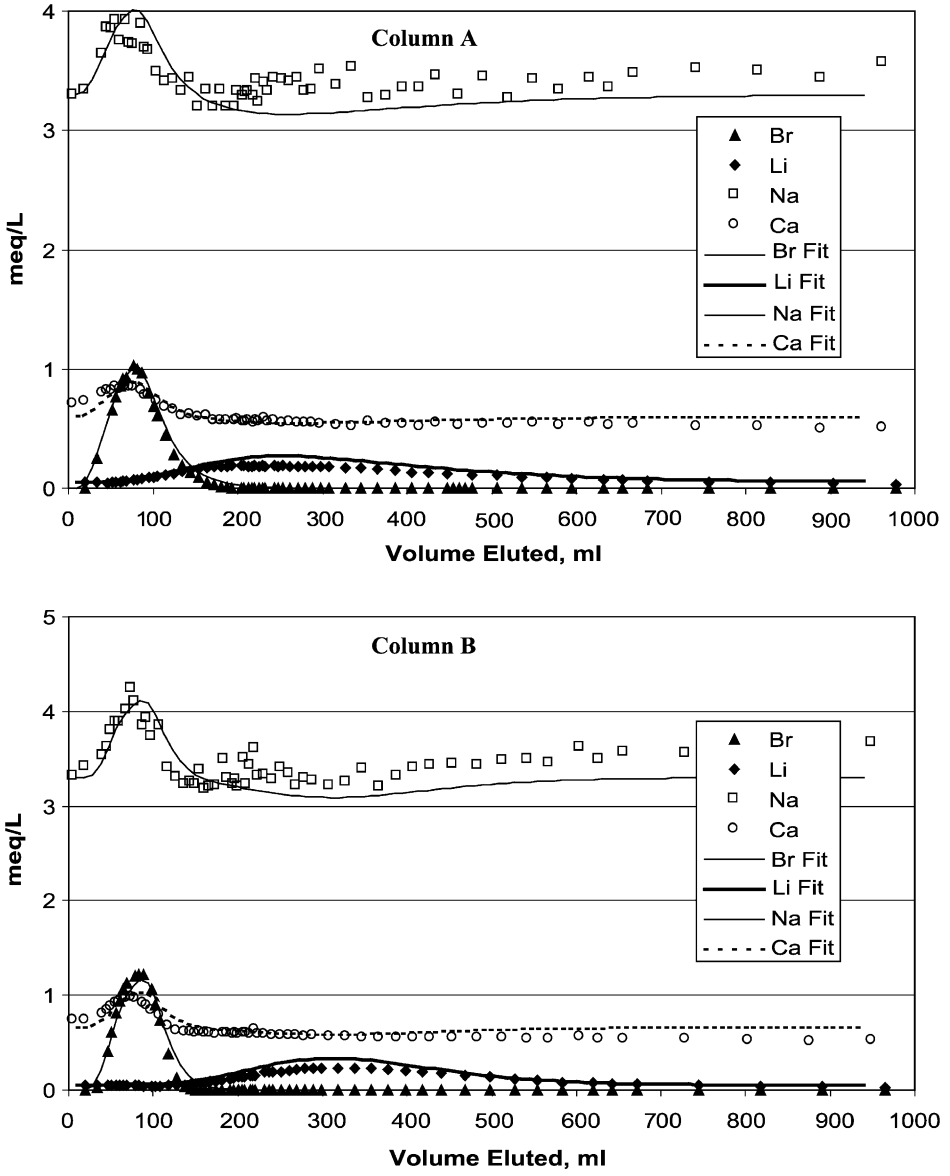

Fig. 7. Column data and MULTRAN fits for experiments with a LiBr injection concentration of 0.0013 M, flow rate 10 ml/h.

displacement of some of the Ca^{2+} in the original material by Na^{+} or Li^{+} might explain the larger Q_1 values and smaller Q_2 values in the subsequent experiments. However, it should be noted that the MULTRAN fits were not extremely sensitive to the Q_1 and Q_2 values, and while the new Q_1 and Q_2 values certainly provided better visual fits to the

later data sets, they were not obtained using a least-squares minimization or optimization algorithm.

The fact that the fluorinated benzoates and bromide transported identically in the columns indicated that there was negligible diffusive mass transfer into stagnant water in the columns, which justified the use of the one-dimensional modeling approach to interpret the column tests. A negligible concentration shift after a flow interruption in the test with 0.0013 M LiBr injection concentration (see Fig. 7, at approximately 500 ml eluted) further verified the lack of diffusive mass transfer in the system.

The partial conservative transport behavior of lithium ion at high injection concentrations (e.g., Fig. 5) is a consequence of both the limited lithium sorption capacity of the alluvium and the requirement that local charge balance must be maintained throughout the columns. When the concentration of lithium ion was a significant fraction of the total cation concentrations in the injection solution (in equivalents/l), some of the lithium exceeded the existing exchange capacity and moved conservatively through the columns with the nonsorbing anion tracers to maintain charge balance. The fraction of early-arriving lithium in the column tests decreased as the LiBr injection concentration decreased, and when the Li^+ concentration was only 24% of the total cation equivalents/l, the lithium was essentially completely retarded (Fig. 7). The lithium responses at the lowest LiBr injection concentration were the only responses that could be adequately modeled assuming a simple linear partition coefficient, K_d (mass sorbed per unit mass of solid/solution concentration), to describe lithium sorption in the columns (fits not shown). Such a model assumes that lithium transport is independent of all other species in solution, which is clearly inaccurate at higher injection concentrations where it becomes a significant fraction of the total cation equivalents in solution.

5.2. Implications for field testing

The lithium transport behavior observed in the column experiments and depicted in Figs. 5–7 has important implications for cross-hole field tracer testing. It is common practice to inject large masses and hence high concentrations of sorbing tracers in field tests because the combination of sorption, dispersion, and dilution can result in very low concentrations at the production well. Large tracer injection masses and concentrations are used to ensure adequate detection and quantification of lithium concentrations at the production well. This strategy means that lithium concentrations may tend to remain quite high for some time (and distance) near the injection well, which could result in some of the lithium moving conservatively through the flow system until the tracer "slug" becomes dispersed and diluted.

There are two possible extremes of sorbing tracer transport in a cross-hole field tracer test that could result in the same observed concentrations at the production well. The first is that the injected tracer slug could disperse and dilute rapidly near the injection well, resulting in a low average concentration throughout the flow system. The second is that the tracer slug could remain relatively concentrated as it moves to the production well and then be diluted in the well bore as a result of mixing with tracer-free water that is also being drawn into the well. There is no way to distinguish between these two extremes, or any intermediate situation, when conservative tracer responses are analyzed. However, the

results and interpretations of the column experiments in this paper suggest that the shape of a lithium breakthrough curve in a cross-hole field tracer test may provide a good indication of whether dilution is occurring early or late in the flow system. If dilution occurs early, a lithium response curve similar to those in Fig. 7 can be expected. However, if dilution occurs late, the lithium response curve may look more like those of Figs. 5 or 6, where there is some asymmetry and conservative transport even though measured concentrations are quite low because of dilution in the production well bore. Knowing whether dilution occurs early or late is important when making comparisons between laboratory and field transport behavior. If concentrations remain high at the pumping well (late dilution), then the lithium may appear to be transporting more conservatively than would be inferred from laboratory batch sorption measurements.

The ability to distinguish between early and late dilution could help refine or constrain estimates of effective flow porosities derived from cross-hole tracer tests. When conservative tracer responses are analyzed, flow porosity estimates are typically based on first, mean, or peak arrival times of conservative tracers. Under ideal radial flow conditions in a confined aquifer, the following equation can be used to estimate effective flow porosity:

$$\varphi = \frac{Q\tau}{\pi L^2 T} \tag{7}$$

where, φ = flow porosity; Q = production flow rate (m^3/h); τ = mean residence time of a conservative tracer (h); L = distance between wells (m); and T = formation thickness (assumed to be well screen length).

If flow heterogeneity exists, causing the flow field to not be radial, then estimates using Eq. (7) will be erroneous. For instance, if most of the flow to the production well is channeled from a direction that does not intersect the tracer slug, then the interwell travel time for the slug can be very long even if flow occurs in only a small fraction of the system volume. In this case, a considerable amount of dilution will occur late in the system (in the production well), and a misleadingly high flow porosity will be deduced from Eq. (7). If an asymmetric lithium response curve with some apparent conservative transport is detected at the production well, the degree of asymmetry in the response can, in principle, be used to estimate the volume that the tracer pulse flowed through within the system. Such an estimate can be obtained by first using MULTRAN in inverse mode to match the shape of the response curve given a known injection pulse concentration, injection duration, alluvium CEC (estimated from laboratory tests), and a longitudinal dispersivity (estimated from the conservative tracer responses). Once a curve shape is matched given these constraints, the flow system volume can be estimated by multiplying the volume of the injection pulse in the field test by the ratio of flow system volume to injection pulse volume assumed in the MULTRAN simulations. An estimate of flow porosity can then be obtained from:

$$\varphi = \frac{V}{\pi L^2 T} \tag{8}$$

where V = volume determined from MULTRAN matches to lithium response.

The flow porosity estimate given by Eq. (8) is independent of tracer travel times, and therefore is not biased by flow channeling resulting from flow system heterogeneity. Such an estimate should be more conservative than one based on tracer travel times. Of course, if the lithium response curve shows no asymmetry, then the method described above can only be used to establish a lower bound for the effective flow porosity. The method relies on the assumption of fast ion exchange kinetics relative to travel times in the flow system (i.e., the local equilibrium assumption), which should be satisfied unless travel times are less than a few hours. Six-hour residence times in the laboratory columns were apparently long enough that the local equilibrium assumption was satisfied. Future work will focus on refining the method and establishing its limitations and uncertainties in field applications.

Acknowledgements

We gratefully acknowledge Steve Chipera of Los Alamos National Laboratory for conducting the X-ray diffraction analyses of the alluvium. This work was supported by the Yucca Mountain Site Characterization Project Office as part of the Civilian Radioactive Waste Management Program. This project is managed by the U.S. Department of Energy, Yucca Mountain Site Characterization Project.

References

Anghel, I., Turin, H.J., Reimus, P.W., in press. Lithium Sorption to Yucca Mountain Tuffs, Appl. Geochem.

Appelo, C.A.J., 1994. Some calculations on multicomponent transport with cation-exchange in aquifers. Ground Water 32 (6), 968–975.

Appelo, C.A.J., 1996. Multicomponent ion exchange and chromatography in natural systems. In: Lichtner, P.C., Steefel, C.I., Oelkers, E.H. (Eds.), Reactive Transport in Porous Media. Rev. Mineral., vol. 34. Mineralogical Society of America, Washington, DC, pp. 193–227.

Appelo, C.A.J., Postma, D., 1993. Geochemistry, Groundwater and Pollution. A.A. Balkema, Rotterdam.

ASTM, 1999. Annual Book of ASTM Standards v. 04.08, Soil and Rock (1): D420-D4914. American Society of Testing and Materials, West Conshohocken, PA, pp. 8–17.

Brunauer, S., Emmett, P.H., Teller, E., 1938. Adsorption of gases in multimolecular layers. J. Am. Chem. Soc. 60, 309–319.

Callahan, T.J., Reimus, P.W., Bowman, R.S., Haga, M.J., 2000. Using multiple experimental methods to determine fracture/matrix interactions and dispersion of nonreactive solutes in saturated volcanic rock. Water Resour. Res. 36 (12), 3547–3558.

Chipera, S.J., Bish, D.L., 1995. Multirefelction RIR and intensity normalizations for quantitative analyses: applications to feldspars and zeolites. Powder Diffr. 10, 47–55.

Lichtner, P.C., 1995. Principles and practice of reactive transport modeling. Mater. Res. Soc. Symp. Proc. 353, 117–130.

Lichtner, P.C., 1996. Continuum formulation of multicomponent-multiphase reactive transport. In: Lichtner, P.C., Steefel, C.I., Oelkers, E.H. (Eds.), Reactive Transport in Porous Media. Rev. Mineral., vol. 34. Mineralogical Society of America, Washington, DC, pp. 1–81.

Liu, C.W., Narasimhan, T.N., 1989. Redox-controlled, multiple-species reactive chemical transport: 1. Model development. Water Resour. Res. 25 (5), 869–882.

Ming, D.W., Dixon, J.B., 1987. Quantitative determination of clinoptilolite in soils by a cation-exchange capacity method. Clays Clay Miner. 35, 463–468.

Newman, J.S., 1973. Electrochemical Systems. Prentice-Hall, Englewood Cliffs, NJ.

Parkhurst, D.L., 1995. User's Guide to PHREEQC—A Computer Program for Speciation, Reaction-Path, Advective Transport, and Inverse Geochemical Calculations. U.S. Geol. Surv. Water Resour. Invest. Rep., Denver, CO 95-4227.

Reimus, P.W., Haga, M.J., Adams, A.I., Callahan, T.J., Turin, H.J., Counce, D.A., 2003. Testing and Parameterizing a Conceptual Solute Transport Model in Saturated Fractured Tuff Using Conservative and Reactive Tracers in Cross-Hole Tracer Tests. J. Contam. Hydrol. 62–63C, 613–636 (this issue).

Robinson, B.A., Viswanathan, H.S., Valocchi, A.J., 2000. Efficient numerical techniques for modeling multicomponent ground-water transport based upon simultaneous solution of strongly coupled subsets of chemical components. Adv. Water Resour. 23, 307–324.

Sullivan, E.J., Reimus, P.W., Ding, M., 2001. Effects of mineralogy, grain size and solution concentration on lithium sorption to saturated alluvium south of Yucca Mountain, Nevada. Abstracts of the American Chemical Society, Environmental Chemistry Division, August 26–30, 2001, vol. 41(2). American Chemical Society, Chicago, IL, pp. 101–105.

TebesStevens, C., Valocchi, A.J., VanBriesen, J.M., Rittmann, B.E., 1998. Multicomponent transport with coupled geochemical and biological reactions: model description and example simulations. J. Hydrol. 209, 8–26.

Turin, H.J., Groffman, A.R., Wolfsberg, L.E., Roach, J.L., Strietelmeier, B.A., in press. Tracer and radionuclide sorption to vitric tuffs of Busted Butte, Nevada, Appl. Geochem.

Valocchi, A.J., Street, R.L., Roberts, P.V., 1981a. Transport of ion-exchanging solutes in groundwater: chromatographic theory and field simulation. Water Resour. Res. 17, 1517–1527.

Valocchi, A.J., Roberts, P.V., Parks, G.A., Street, R.L., 1981b. Simulation of the transport of ion-exchanging solutes using laboratory-determined chemical parameter values. Ground Water 19, 600–607.

Yeh, G.T., Tripathi, V.S., 1988. HYDROGEOCHEM: A Coupled Model of Hydrological Transport and Geochemical Equilibrium of Multi-Component Systems, Rep. ORNL-6371. Oak Ridge National Laboratory, Oak Ridge, TN.

Yeh, G.T., Tripathi, V.S., 1989. A critical evaluation of recent developments of hydrogeochemical transport models of reactive multichemical components. Water Resour. Res. 25, 93–108.